Science Advances
AAAS

Supplementary Materials for

In vivo hitchhiking of immune cells by intracellular self-assembly of bacteria-mimetic nanomedicine for targeted therapy of melanoma

Cheng Gao, Qingfu Wang, Junyan Li, Cheryl H. T. Kwong, Jianwen Wei, Beibei Xie, Siyu Lu, Simon M. Y. Lee*, Ruibing Wang*

*Corresponding author. Email: rwang@um.edu.mo (R.W.); simonlee@um.edu.mo (S.L.)

Published 11 May 2022, *Sci. Adv.* **8**, eabn1805 (2022)
DOI: 10.1126/sciadv.abn1805

This PDF file includes:

Figs. S1 to S17

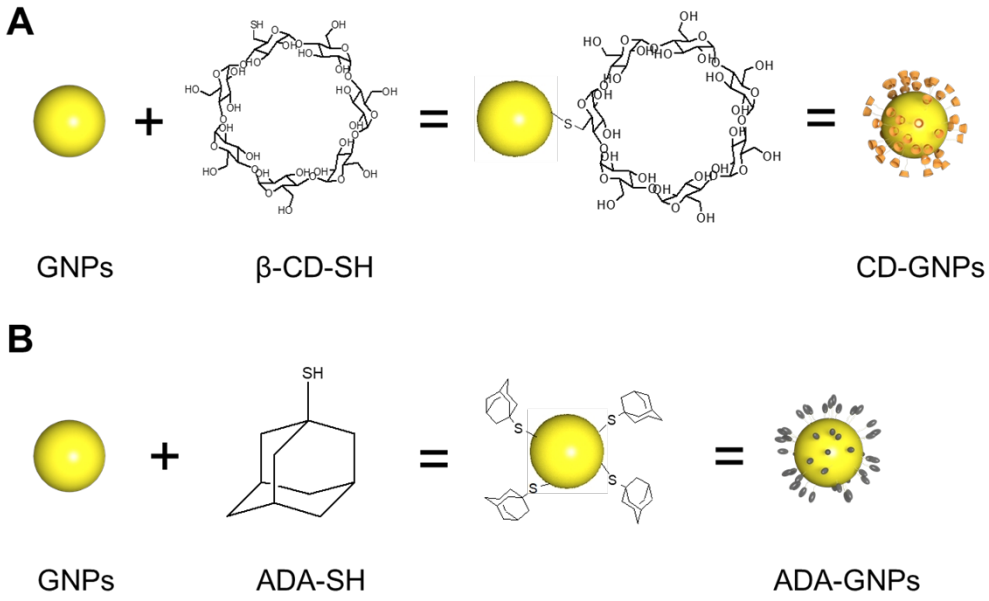

Fig. S1. Synthetic process of CD-GNPs (A) and ADA-GNPs (B).

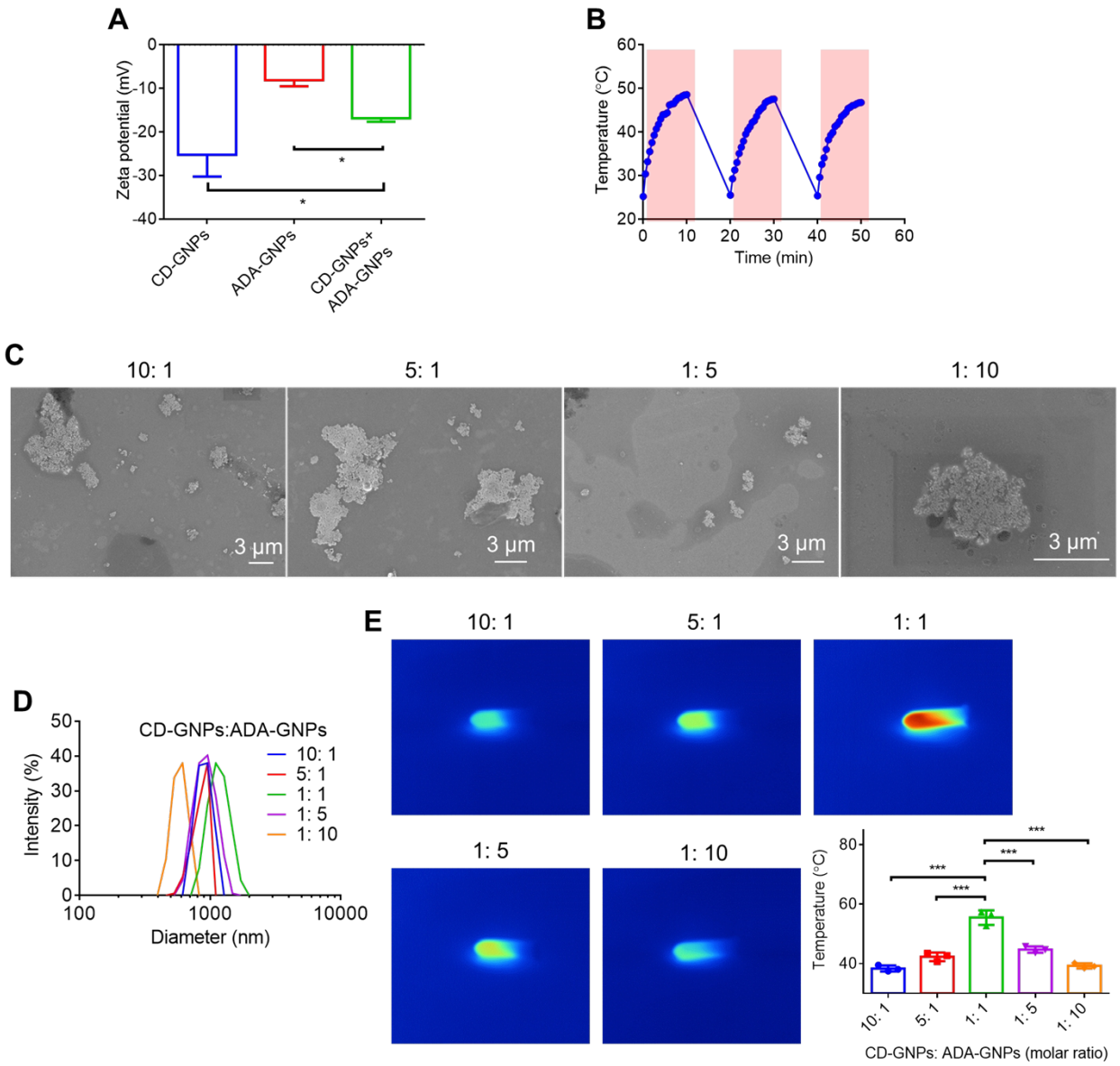

Fig. S2. **Characterizations of GNP aggregates.** (**A**) Zeta potential of CD-GNPs, ADA-GNPs and the mixture of CD-GNPs and ADA-GNPs. (**B**) Photothermal property of the mixture of CD-GNPs and ADA-GNPs (at a total concentration of 0.2 mg/mL GNPs) under NIR irradiation with 808 nm laser (0.5W/cm^2) for 10 min, and repeated for 3 time with an interval of 10 min. (**C**) SEM images of GNP aggregates from different GNP molar ratios between CD-GNPs and ADA-GNPs (10:1, 5:1, 1:5, 1:10). (**D**) Diameters of GNP aggregates from different GNP molar ratios of CD-GNPs and ADA-GNPs (10:1, 5:1, 1:1, 1:5, 1:10). (**E**) The photothermal imaging and temperature after NIR irradiation for 5 min. The experiments were repeated for three times (n = 3) and data was presented as mean ± s.d. All statistical analyses were conducted using One-Way ANOVA. *P≤0.05, **P≤0.01, and ***P≤0.001.

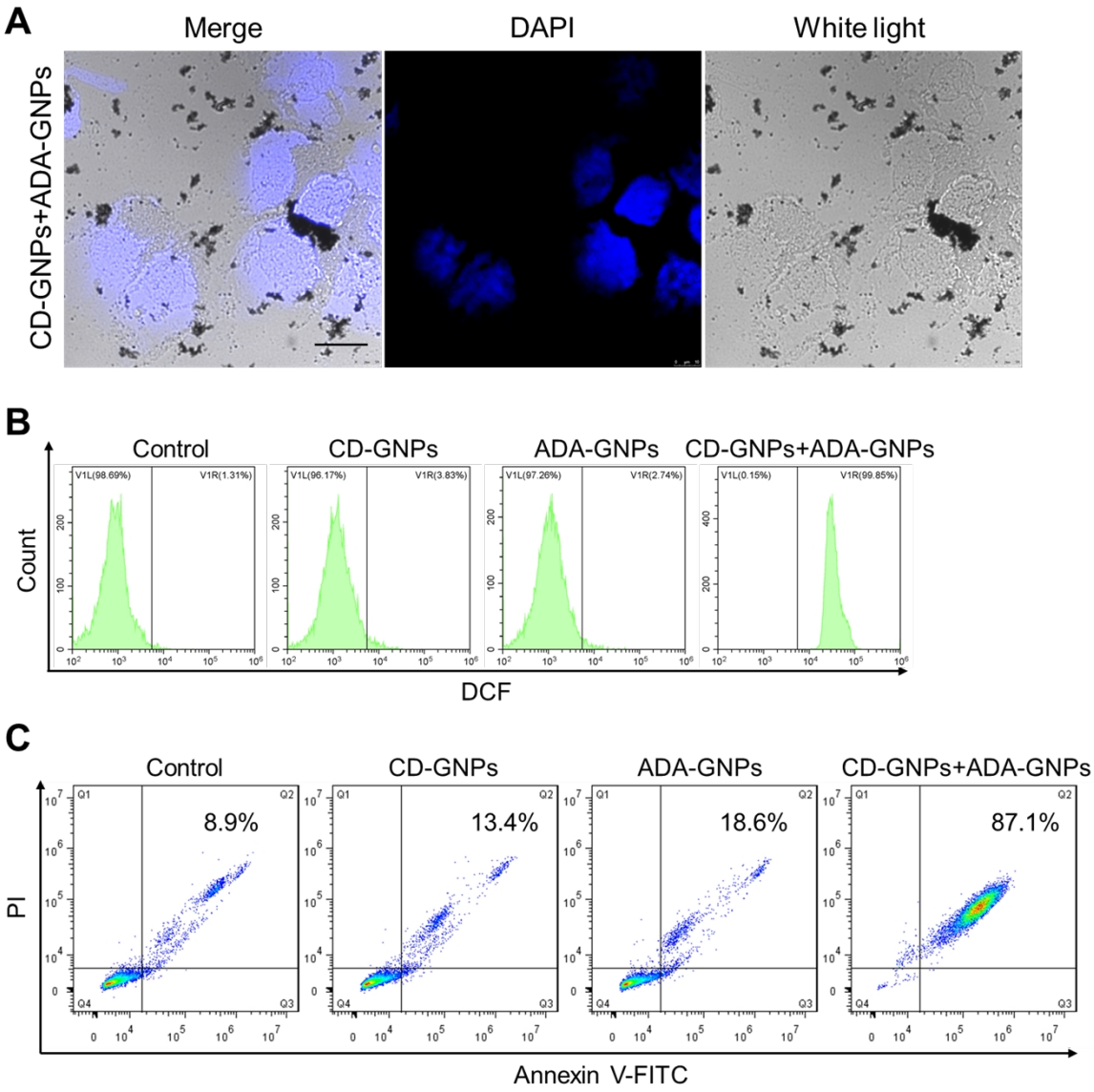

Fig. S3. PTT induced growth inhibition of B16 cells. (**A**) After incubation with GNP aggregates for 3 h, B16 cells were imaged by CLSM. Scale bar, 20 μm. (**B** and **C**) Flow cytometry data on the ROS generation (B) and apoptosis rate (C) of B16 cells after NIR irradiation with 808 nm laser (0.5W/cm^2) for 5 min.

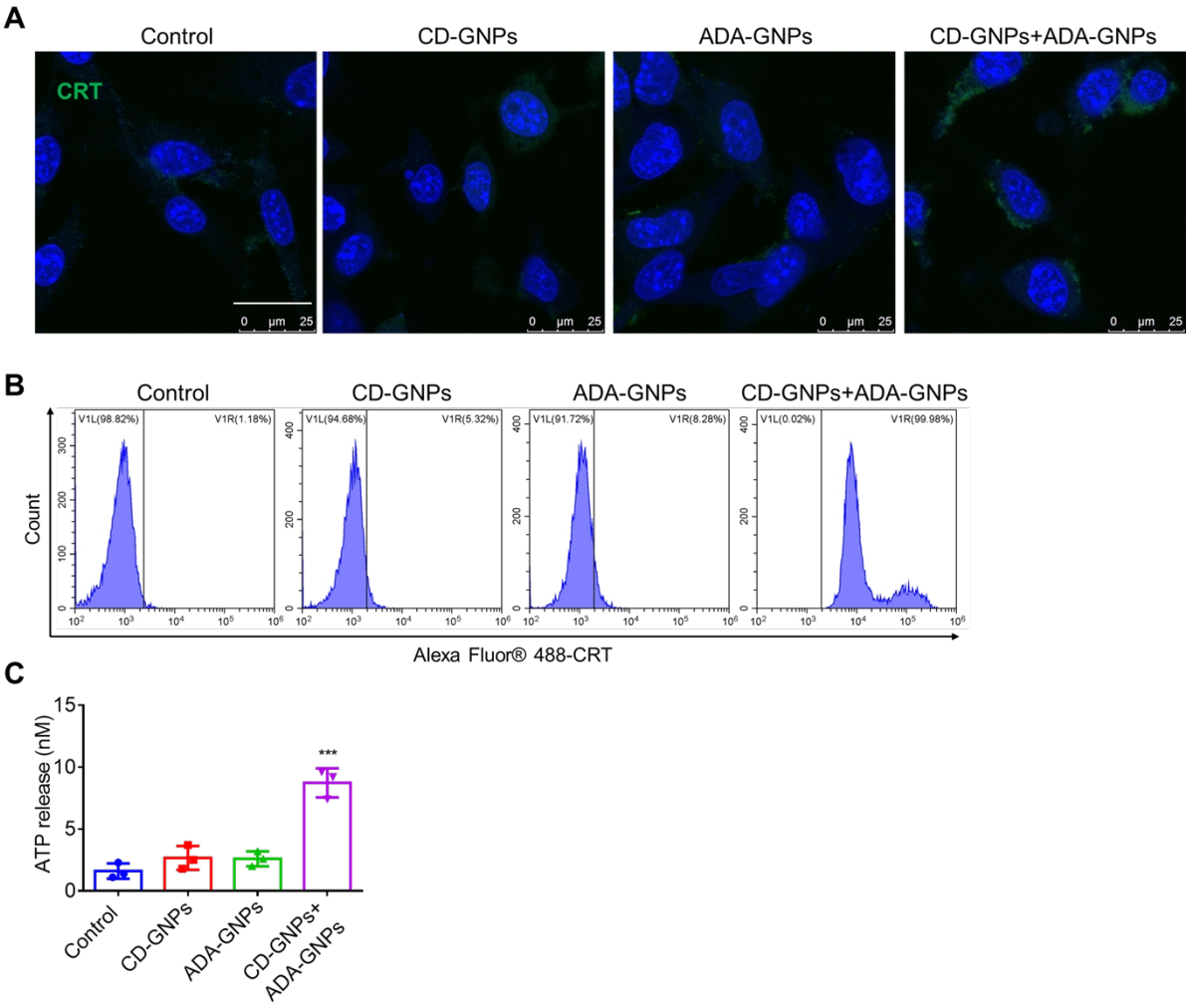

Fig. S4. PTT of GNP aggregates induced ICD of B16 cells. (**A** and **B**) After treatment with of CD-GNPs, ADA-GNPs and the mixture of CD-GNPs and ADA-GNPs at a total concentration of 0.2 mg/mL GNPs for 6 h, B16 cells were irradiated with 808 nm laser (0.5W/cm^2) for 10 min and incubated for further 24 h. B16 cells were subsequently incubated with Alexa Fluor® 488-CRT antibody and imaged by CLSM (A), and quantified by flow cytometry (B). (**C**) Cell culture medium was collected for the determination of ATP by Elisa assays. The experiments were repeated for three times (n = 3) and data was presented as mean ± s.d. All statistical analyses were conducted using One-Way ANOVA. *P≤0.05, **P≤0.01, and ***P≤0.001.

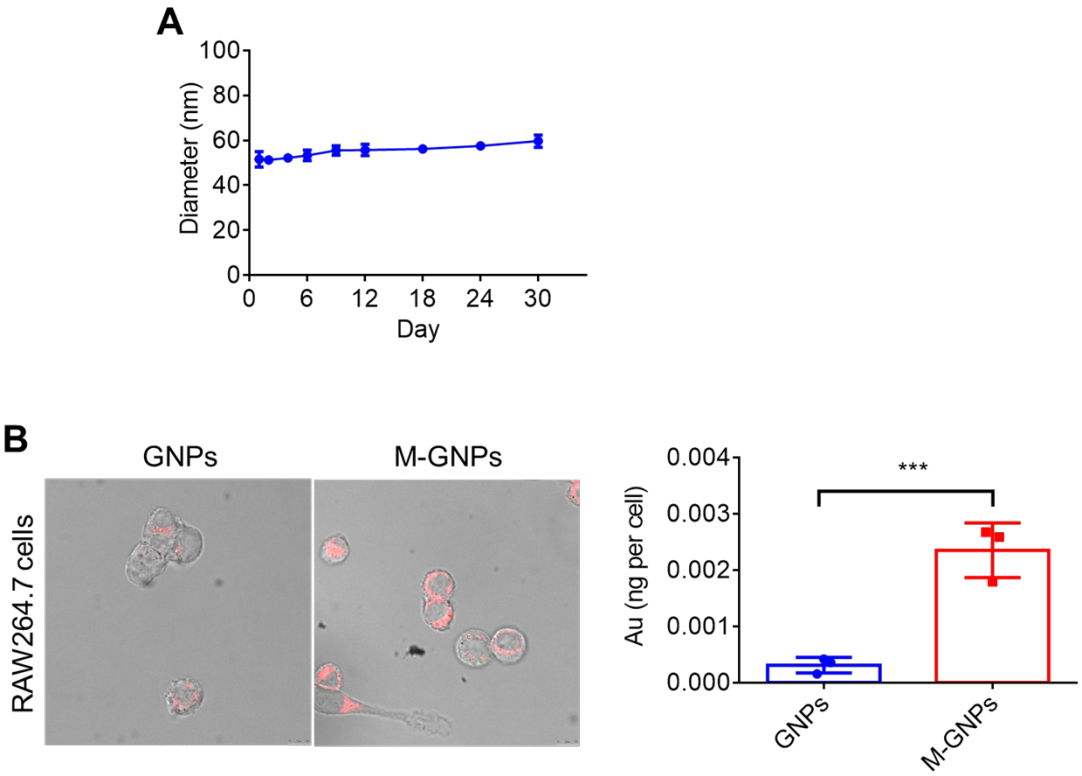

Fig. S5. **Characterization of M-GNPs**. (**A**) The diameter changes of M-GNPs after storage for 1 month, determined by DLS. (**B**) Fluorescence imaging on the intracellular uptake of GNPs and M-GNPs by RAW264.7 cells after pre-incubation with cytochalasin for 3 h, and the quantitative analysis on the intracellular Au content by ICP-MS.

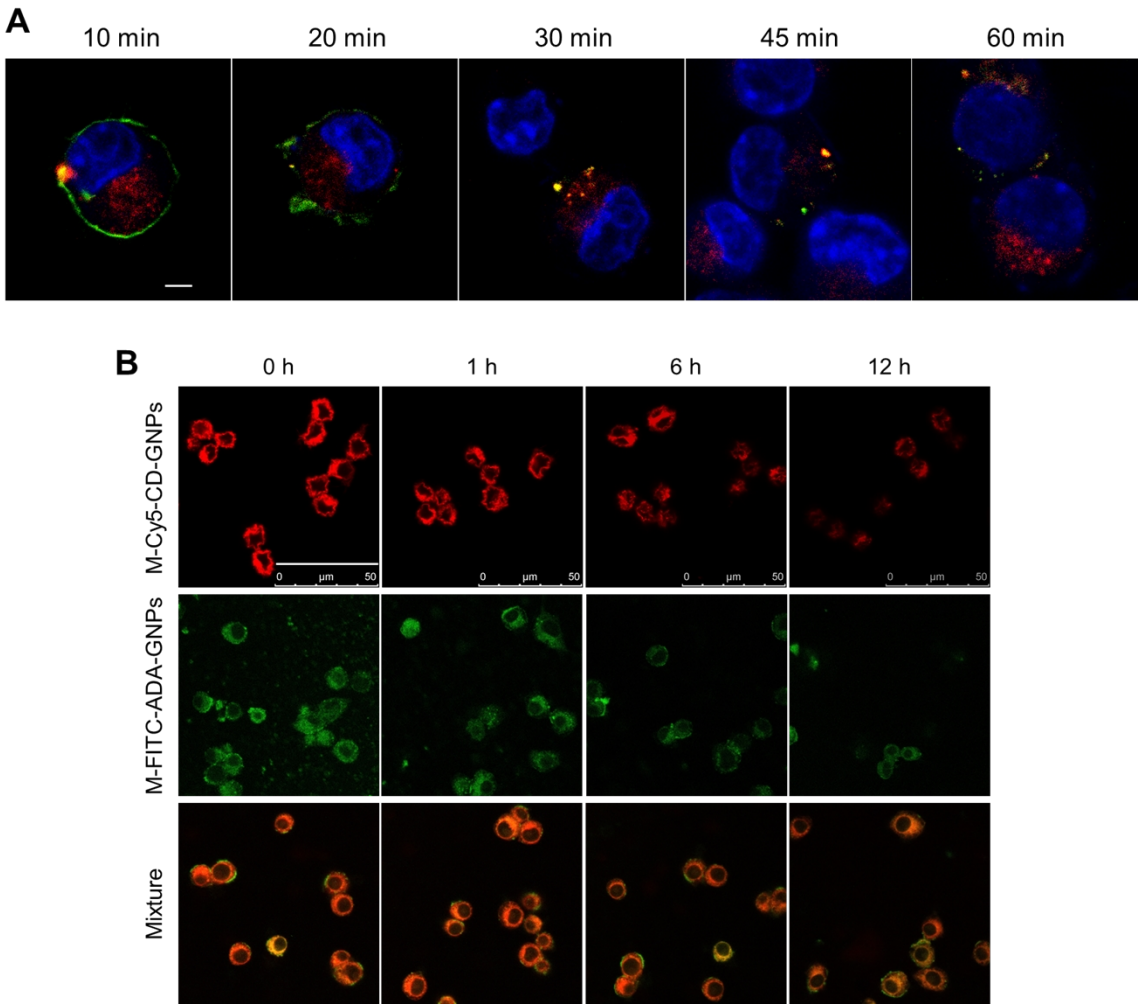

Fig. S6. Degradation of OMVs and efflux behavior of macrophage towards Mixture. (**A**) OMVs were stained with DiO to prepare Mixture, and the degradation process of coated OMVs in macrophage was detected by CLSM after incubation for different times (10 min, 20 min, 30 min, 45 min and 60 min). (**B**) After treatment with the mixture of M-FITC-ADA-GNPs and M-Cy5-CD-GNPs for 6 h, RAW264.7 cells were incubated in fresh media for different durations (1, 6 and 12 h), and imaged by CLSM. Scale bar: 50 μm. The experiments were repeated for three times (n = 3).

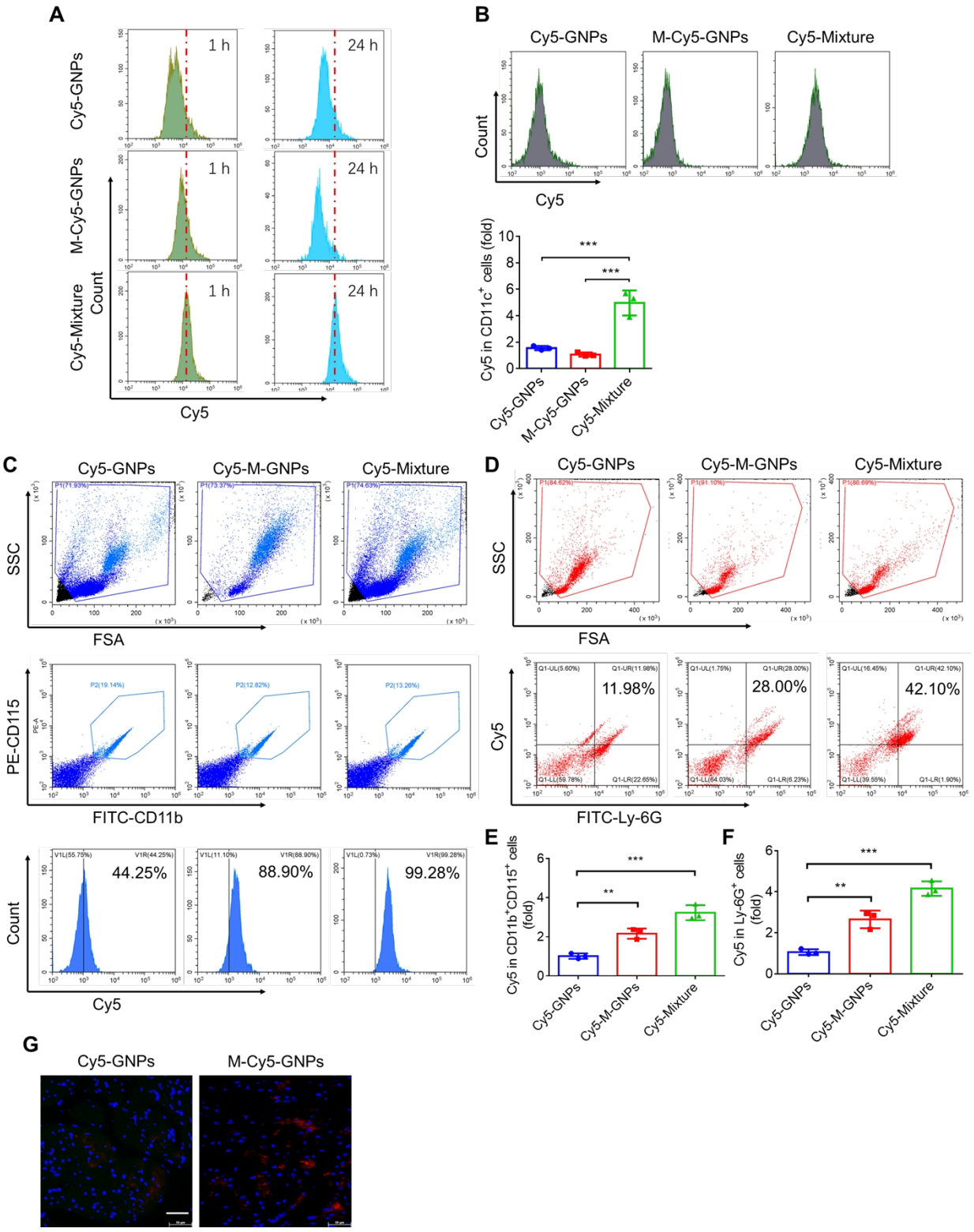

Fig. S7. Selective phagocytosis of GNPs, M-GNPs and Mixture by leukocytes. (**A**) Melanoma mice were respectively treated with Cy5-GNPs, M-Cy5-GNPs and Cy5-Mixture at a dose of 0.5 mg/kg Cy5 for 24 h, and the quantitative analysis on the Cy5 fluorescence intensity of WBCs

(leukocytes) was conducted by flow cytometry. (**B**) Flow cytometry analysis of the Cy5 fluorescence intensity of blood $CD11c^+$ cells. (**C** and **D**) Melanoma mice were respectively treated with Cy5-GNPs, M-Cy5-GNPs and Cy5-Mixture at a dose of 0.5 mg/kg Cy5 for 24 h, and the flow cytometry analysis of Cy5 fluorescence was conducted in the collected circulating neutrophils (Ly-$6G^+$ cells) (C) and monocytes ($CD11b^+CD115^+$ cells) (D) from the blood at 24 h after administration. (**E** and **F**) Quantitative results of Cy5 in the circulating neutrophils (Ly-$6G^+$ cells) (E) and monocytes ($CD11b^+CD115^+$ cells) (F). (**G**) Fluorescent section analysis of the tumor collected from mice treated with M-Cy5-GNPs for 24 h. Red: Cy5 labeled GNPs. The experiments were repeated for three times ($n = 3$) and data was presented as mean ± s.d. All statistical analyses were conducted using One-Way ANOVA. *$P \leq 0.05$, **$P \leq 0.01$, and ***$P \leq 0.001$.

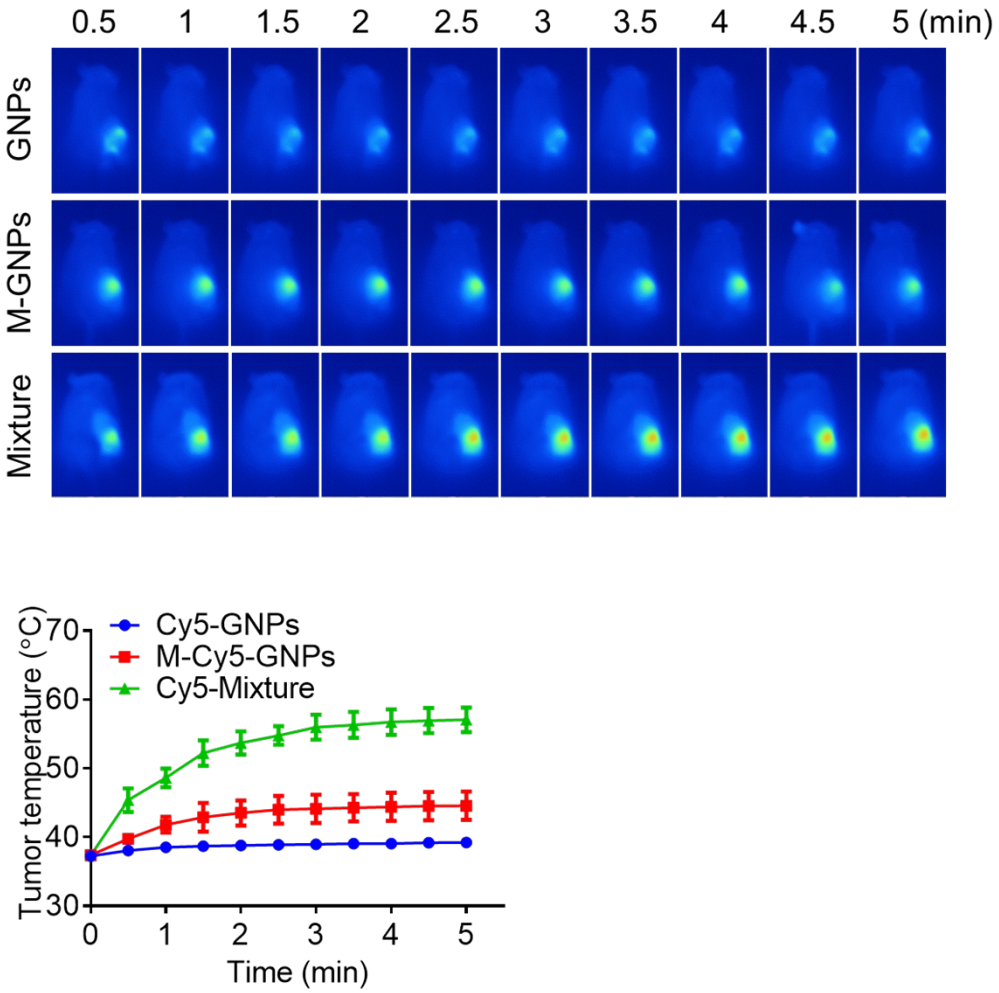

Fig. S8. Photothermal efficiency of Mixture in melanoma mice after administration for 1 h. After i.v. administration with GNPs, M-GNPs and Mixture at a dose of 10 mg/Kg GNPs for 1 h, the photothermal imaging was conducted on melanoma mice under NIR irradiation (808 nm) for 5 min at a power of 0.5 W/cm^2, and temperature in the tumor sites was recorded. The experiments were repeated for three times (n = 3) and data was presented as mean ± s.d.

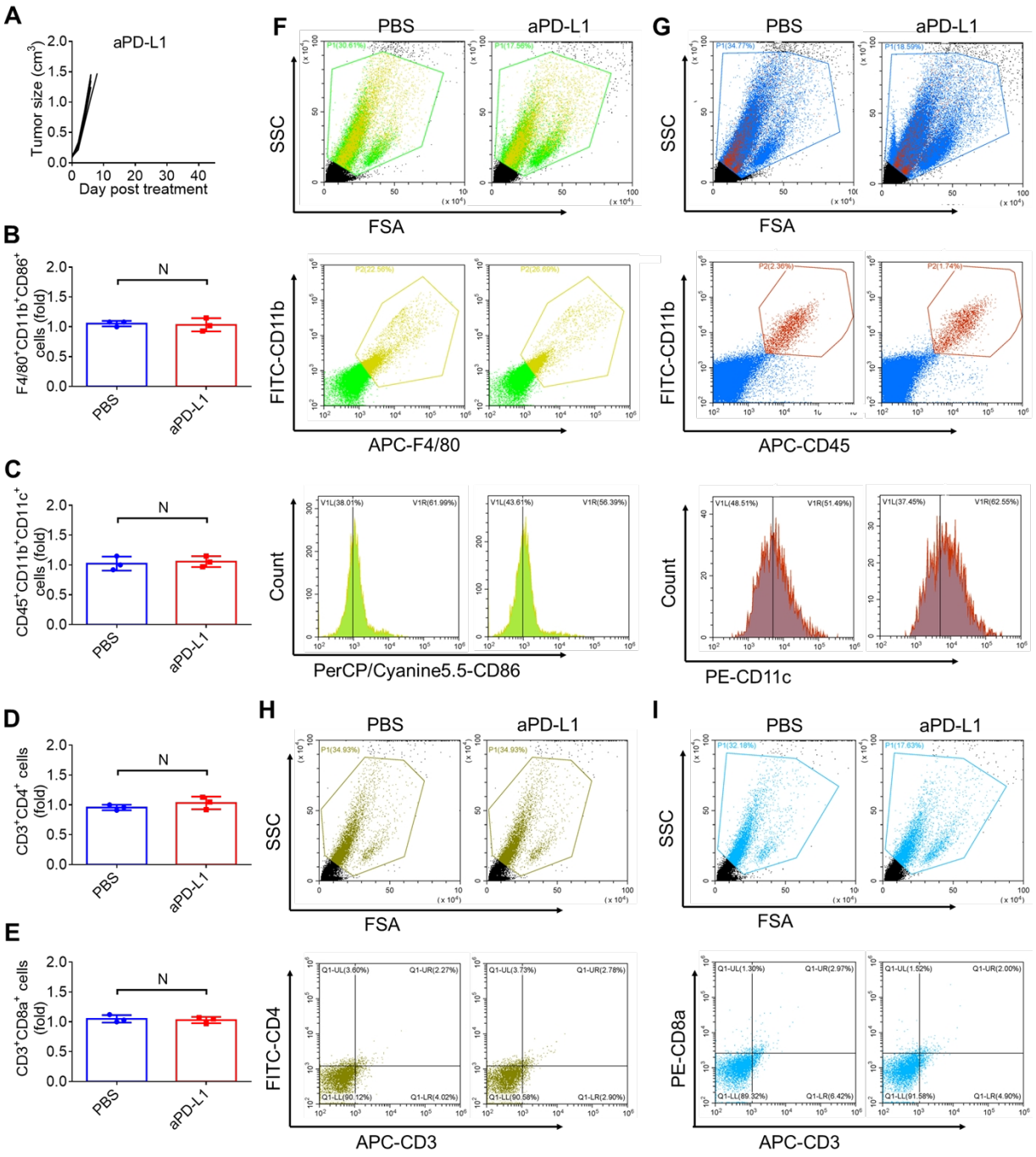

Fig. S9. **Poor antitumor immunotherapy of aPD-L1 against melanoma.** (**A**) Melanoma mice were treated with PBS, and 8 μg aPD-L1/mouse once every 3 days for a total of 5 doses, and the tumor size was recorded. (**B** to **E**) The tumor tissues were collected after administration for 7 days, and flow cytometry analysis was conducted on the infiltration of $F4/80^+CD11b^+CD86^+$ cells (B), $CD45^+CD11c^+$ cells (C), $CD3^+CD4^+$ cells (D), and $CD3^+CD8a^+$ cells (E) in the tumor tissues. (**F** to **I**) Gating strategy of flow cytometry analysis on $F4/80^+CD11b^+CD86^+$ cells (F), $CD45^+CD11b^+CD11c^+$ cells (G), $CD3^+CD4^+$ T cells (H) and $CD4^+CD8^+$ T cells (I). The experiments were repeated for three times and data was presented as mean ± s.d. All statistical analyses were performed using One-Way ANOVA. *P≤0.05, **P≤0.01, and ***P≤0.001.

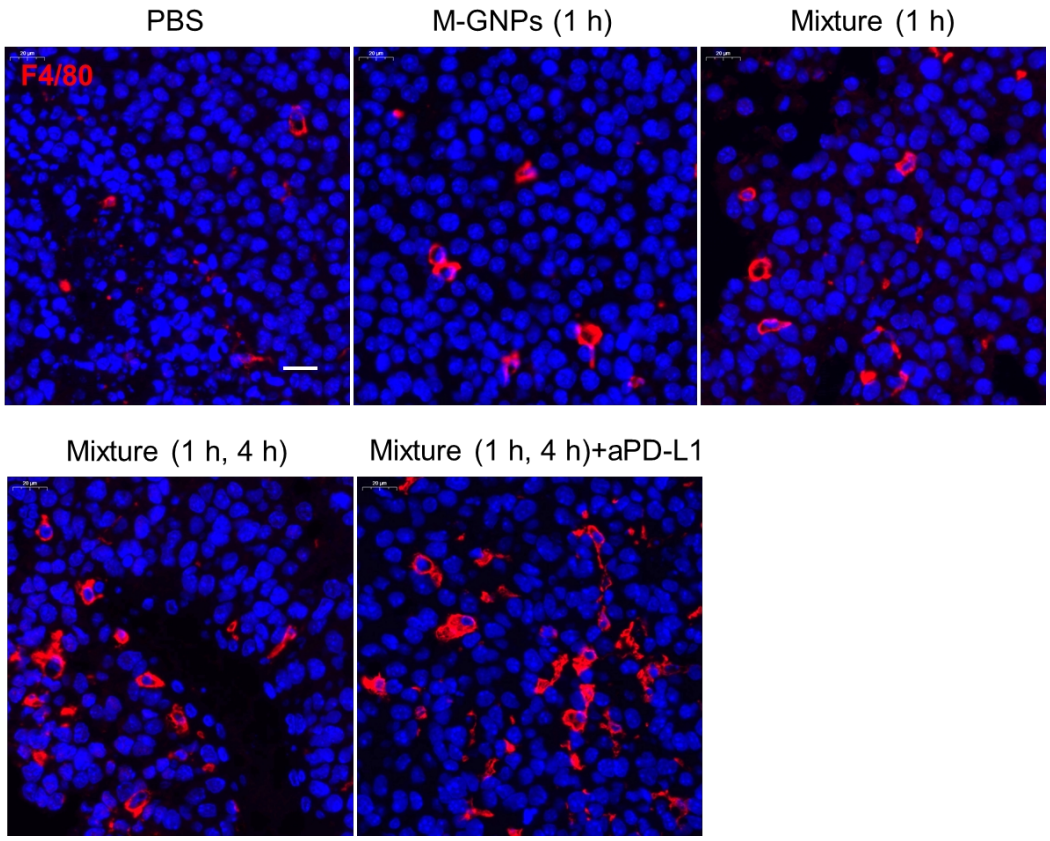

Fig. S10. Fluorescence imaging on tumor filtration of F4/80$^+$ cells. Melanoma mice were treated with PBS, M-GNPs (1 h), Mixture (1 h), Mixture (1 h, 4 h), and Mixture (1 h, 4 h) assisted by 8 μg aPD-L1/mouse once every 3 days for a total of 5 doses (Mixture (1 h, 4h)+aPD-L1), at a same dose of 10 mg/Kg GNPs, and immunofluorescence analysis on the filtration of F4/80$^+$ cells in the tumor tissues collected from mice after administration for 7 days.

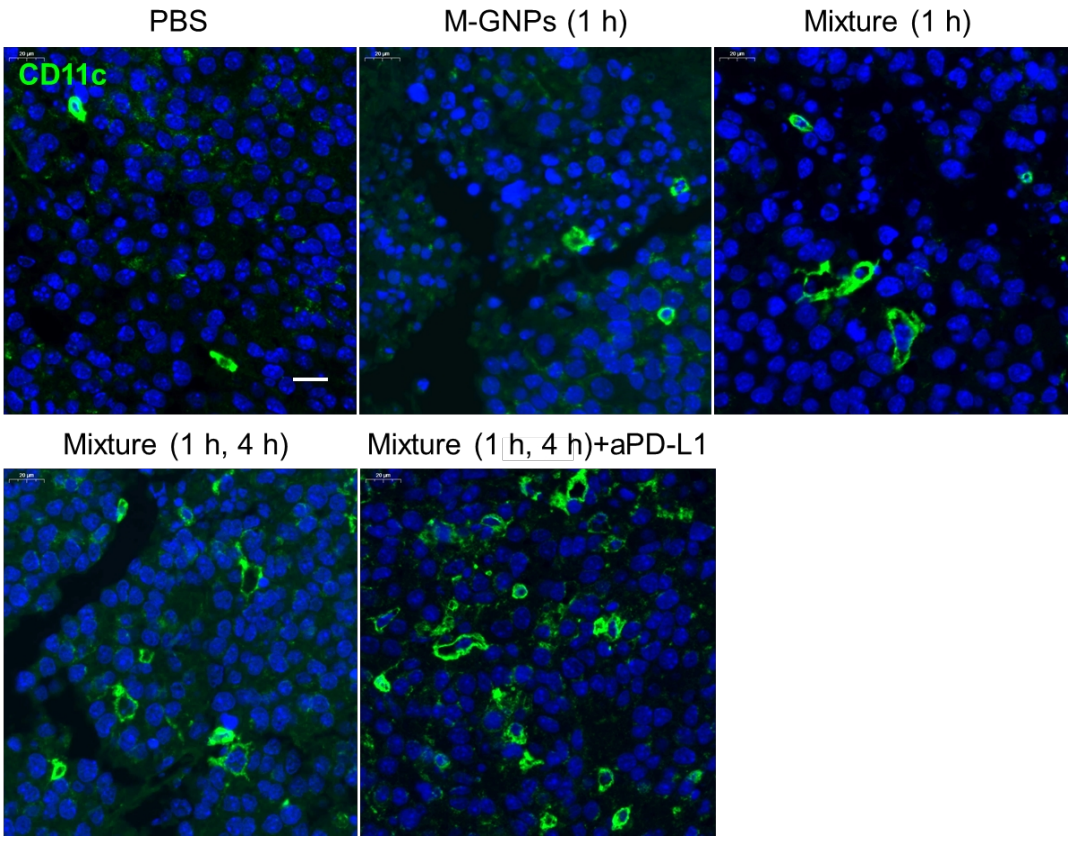

Fig. S11. Fluorescence imaging on tumor filtration of CD11c$^+$ cells. Melanoma mice were treated with PBS, M-GNPs (1 h), Mixture (1 h), Mixture (1 h, 4 h), and Mixture (1 h, 4 h) assisted by 8 μg aPD-L1/mouse once every 3 days for a total of 5 doses (Mixture (1 h, 4h)+aPD-L1), at a same dose of 10 mg/Kg GNPs, and immunofluorescence analysis on the filtration of CD11c$^+$ cells in the tumor tissues collected from mice after administration for 7 days.

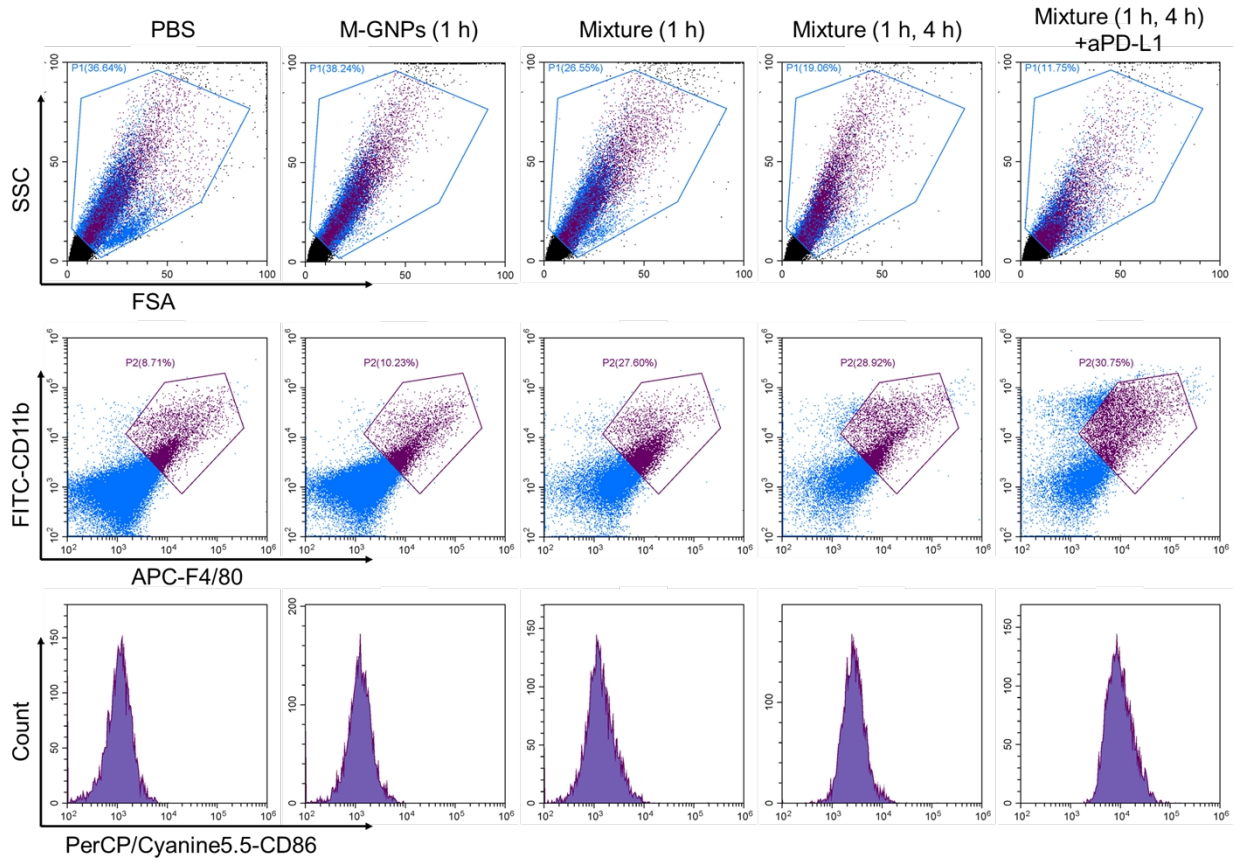

Fig. S12. Gating strategy of flow cytometry analysis on M1 macrophage. Melanoma mice were treated with PBS, M-GNPs (1 h), Mixture (1 h), Mixture (1 h, 4 h), and Mixture (1 h, 4 h) assisted by 8 μg aPD-L1/mouse once every 3 days for a total of 5 doses (Mixture (1 h, 4h)+aPD-L1), at a same dose of 10 mg/Kg GNPs, and flow cytometry analysis on M1 macrophage ($F4/80^+CD11b^+CD86^+$ cells) in the tumor tissue was conducted after administration for 7 days (n=3).

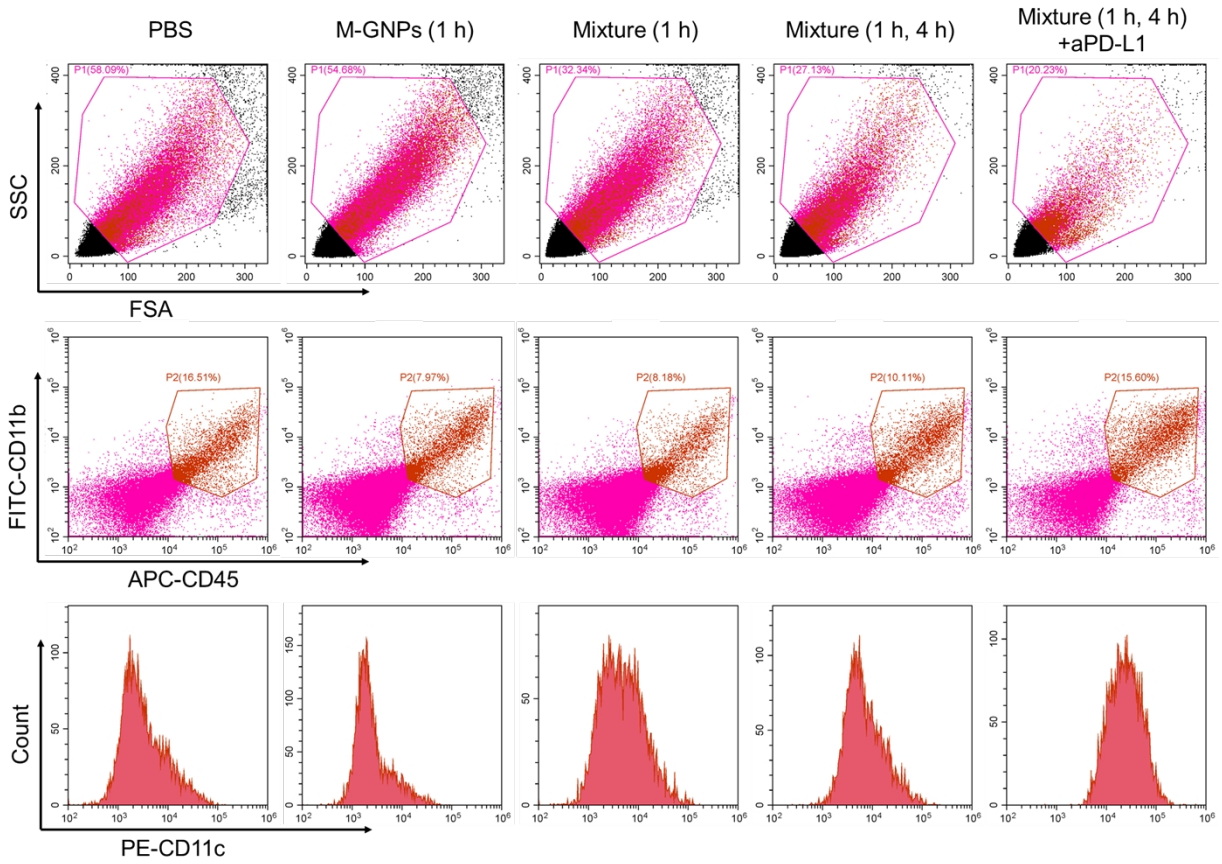

Fig. S13. Gating strategy of flow cytometry analysis on DCs. Melanoma mice were treated with PBS, M-GNPs (1 h), Mixture (1 h), Mixture (1 h, 4 h), and Mixture (1 h, 4 h) assisted by 8 μg aPD-L1/mouse once every 3 days for a total of 5 doses (Mixture (1 h, 4h)+aPD-L1), at a same dose of 10 mg/Kg GNPs, and flow cytometry analysis on DCs ($CD45^+CD11b^+CD11c^+$ cells) in the tumor tissue was conducted after administration for 7 days (n=3).

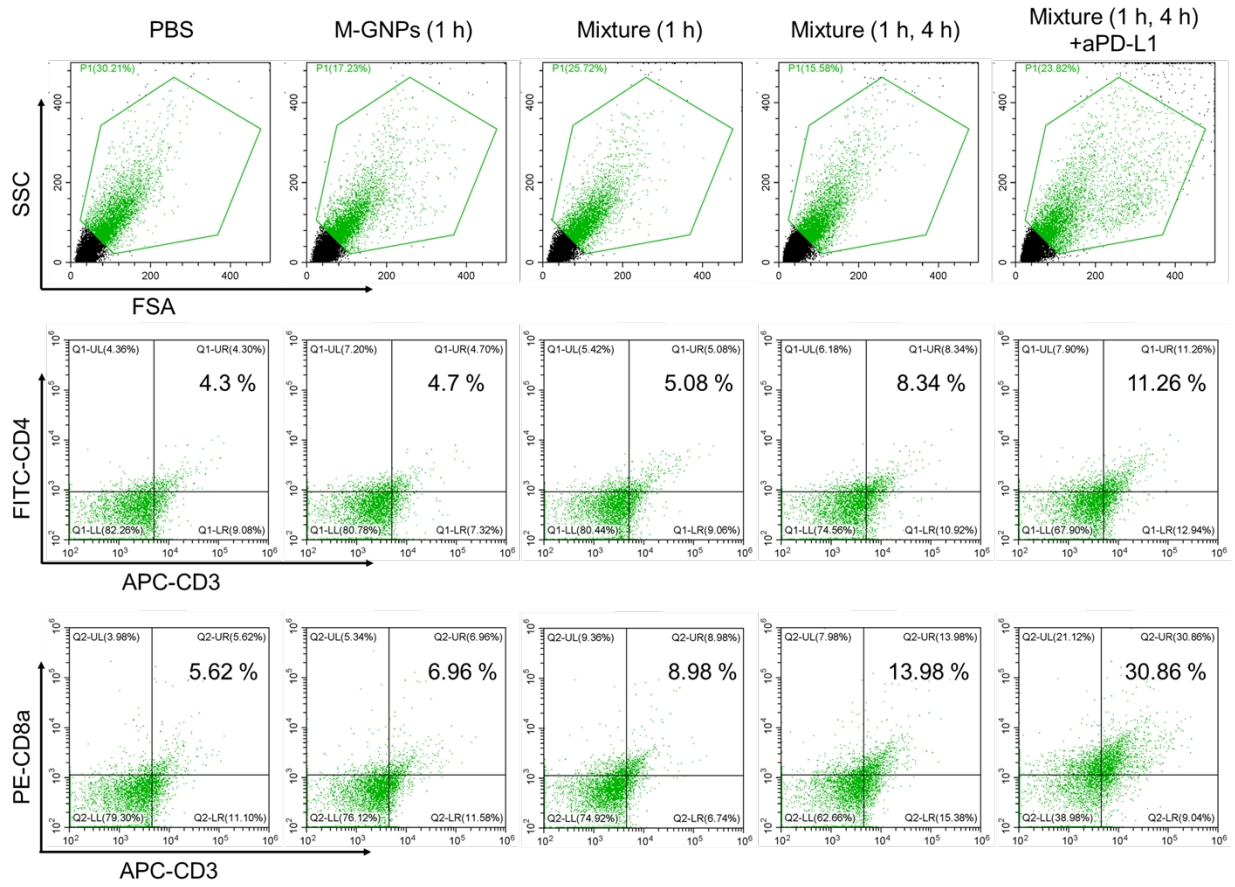

Fig. S14. Gating strategy of flow cytometry analysis on $CD4^+$ T cells and $CD8^+$ T cells. Melanoma mice were treated with PBS, M-GNPs (1 h), Mixture (1 h), Mixture (1 h, 4 h), and Mixture (1 h, 4 h) assisted by 8 μg aPD-L1/mouse once every 3 days for a total of 5 doses (Mixture (1 h, 4h)+aPD-L1), at a same dose of 10 mg/Kg GNPs and flow cytometry analysis on $CD4^+$ T cells ($CD3^+CD4^+$ cells) and $CD8^+$ T cells ($CD3^+CD8a^+$ cells) in the tumor tissue was conducted after administration for 7 days (n=3).

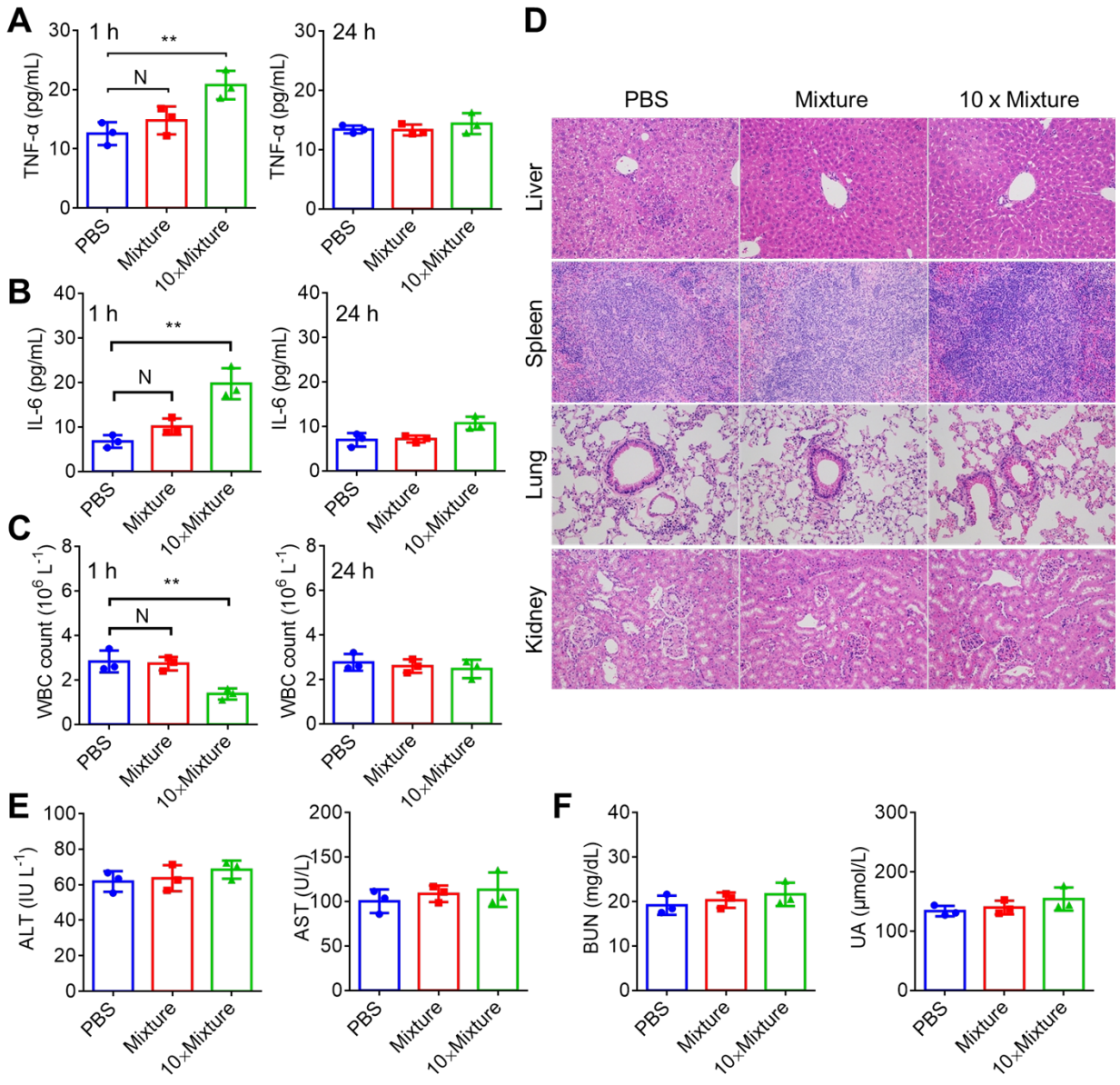

Fig. S15. In vivo safety evaluation of Mixture on C57BL/6 mice. (**A** and **B**) The mice were i.v. administered with PBS, Mixture, and 10-fold of Mixture (20 mg mL^{-1} GNPs and 60.8 μg mL^{-1} LPS), the level of TNF-α (A) and IL-6 (B) in serum were analyzed by Elisa assay after administration for 1 h and 24 h, respectively. (**C**) The number of WBCs in blood was measured by hemocytometer after administration for 1 h and 24 h, respectively. (**D** to **F**) After administration for 24 h, HE staining was conducted in the heart, liver, spleen, lungs, and kidneys (D), and the level of ALT, AST (E), BUN and UA (F) in the blood serum were analyzed. The experiments were repeated for three times (n = 3) and data was presented as mean ± s.d. All statistical analyses were conducted using One-Way ANOVA. *P≤0.05, **P≤0.01, and ***P≤0.001.

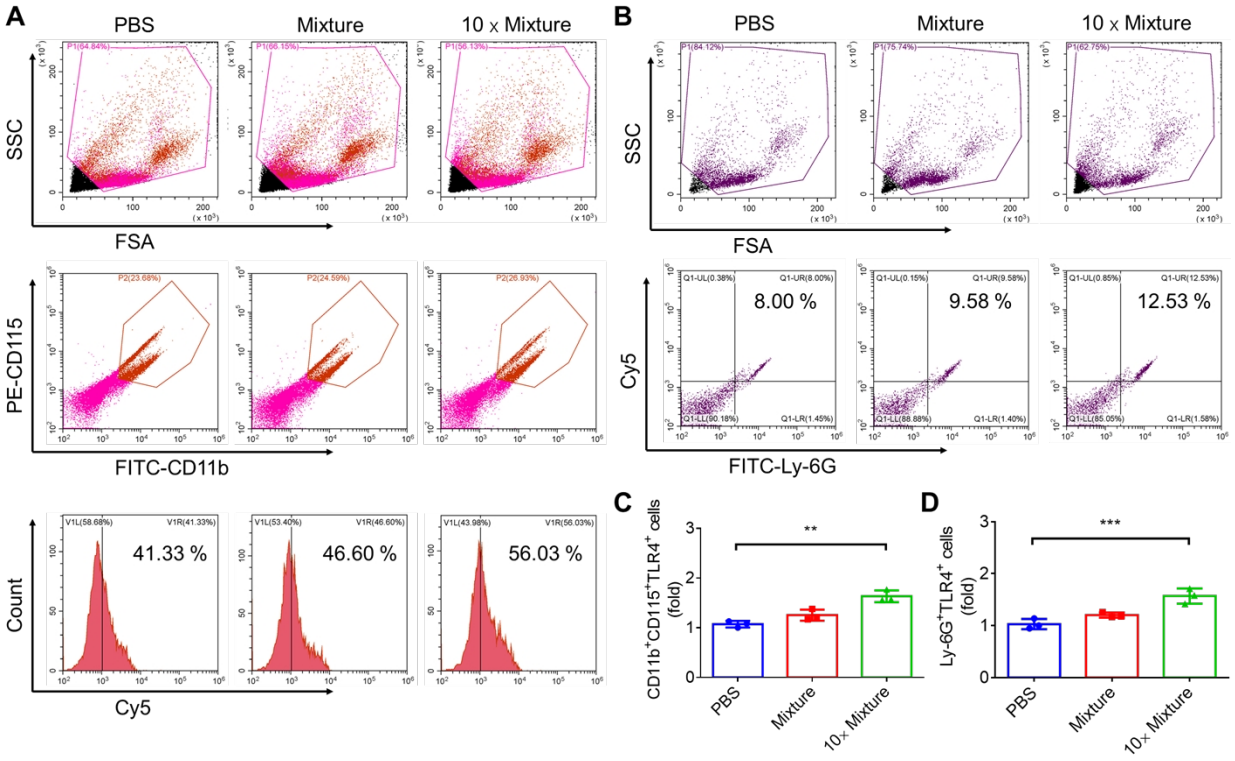

Fig. S16. Polarization of the circulating leukocytes by Mixture. The mice were i.v. administered with PBS, Mixture, and 10-fold Mixture for 24 h, and the percent of Ly-6G$^+$TLR4$^+$ cells and CD11b$^+$CD115$^+$TLR4$^+$ cells in the blood was analyzed by flow cytometry. (**A** and **B**) The gating strategy of Ly-6G$^+$TLR4$^+$ cells and CD11b$^+$CD115$^+$TLR4$^+$ cells. (**C** and **D**) The quantitative results of Ly-6G$^+$TLR4$^+$ cells and CD11b$^+$CD115$^+$TLR4$^+$ cells.

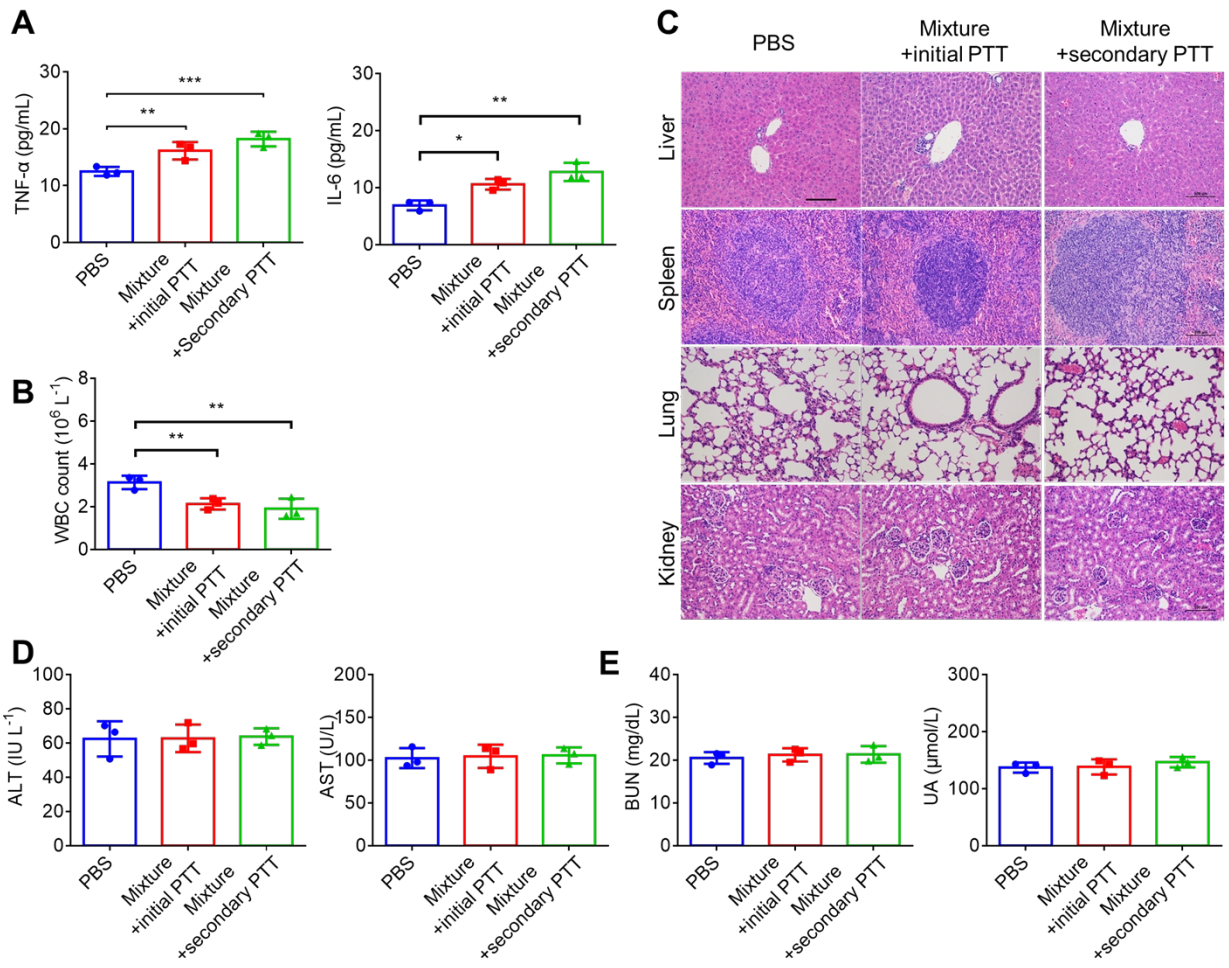

Fig. S17. In vivo safety evaluation of Mixture treated C57BL/6 mice followed by initial PTT treatment and secondary PTT treatment. (**A**) The mice were i.v. administered with Mixture for 1 h, and followed by initial PTT treatment and secondary PTT treatment. After both treatment for 3 h, the level of TNF-α and IL-6 in serum were analyzed by Elisa assays. (**B**) The number of WBCs in blood was measured by hemocytometer. (**C** to **E**) HE staining was conducted in the heart, liver, spleen, lungs, and kidneys (C), and the level of ALT, AST (D), BUN and UA (E) in the blood serum were analyzed. Scale bar: 100 μm. The experiments were repeated for three times (n = 3) and data was presented as mean ± s.d. All statistical analyses were conducted using One-Way ANOVA. *P≤0.05, **P≤0.01, and ***P≤0.001.